Proceedings of the 11th World Congress on Mechanical, Chemical, and Material Engineering (MCM'25)

Paris, France - August, 2025 Paper No. ICMIE 136 DOI: 10.11159/icmie25.136

Design, Kinematic Analysis, and Prototyping of a Six-Bar Linkage-Based Legged Robot

Behbehani Danah, AlGhashem Noor, AlAjmi Hanoof, Fathaldin Saleemah, Hussain Fatemah, Prasad Benrose and Gazo-Hanna Eddie*

College of Engineering and Technology, American University of the Middle East Egaila 54200, Kuwait

54080@aum.edu.kw, 54096@aum.edu.kw, 54639@aum.edu.kw, 59457@aum.edu.kw, 53330@aum.edu.kw, Benrose.prasad@aum.edu.kw, eddie-hanna@aum.edu.kw

*Corresponding author: Eddie-hanna@aum.edu.kw

Abstract - This study focuses on the development and analysis of a novel six-bar linkage mechanism with a single degree of freedom, incorporating an integrated skew pantograph. Using GIM software, the mechanism's dimensions were synthesized to generate an optimized foot trajectory, ensuring stability, reduced energy consumption, and smooth motion. A comprehensive kinematic analysis simulated the leg's motion, while SolidWorks was employed for stress analysis and topology optimization. The results demonstrate the mechanism's potential for applications in robotics, all-terrain vehicles, and agricultural machinery. This design combines compactness with enhanced coupler curve amplification, providing improved performance and adaptability in challenging environments.

Keywords: Legged robot; six-Bar linkage; skew pantograph; robotics; planar mechanism

1. Introduction

The study of leg mechanisms, particularly in how they move, encompasses analyzing the positions, velocities, and accelerations of their components without considering the forces or torques driving such movements. These mechanisms are composed of various components linked by joints, which limit the movement possibilities between them. Such a configuration ensures that the movement of each component is interdependent, illustrating a fundamental principle of kinematics, which focuses on the geometry of motion.

Among the diverse leg mechanisms utilized in walking machines, the Klann mechanism and Jansen linkages stand out for their widespread application. The Klann mechanism [1], [2], [3], a pivotal example of an eight-bar kinematic chain, replicates the locomotion of legged animals and serves as an alternative to traditional wheels. It comprises a frame, cranks, a pair of grounded rockers, and two couplers connected by pivot joints. This design offers notable benefits for walking machines, such as the ability to come over obstacles like curbs and stairs, and access areas challenging for wheeled mechanisms without the need for sophisticated control systems or extensive actuation devices.

The Jansen linkage [1], [2], [3], [4], renowned for its ability to produce a fluid walking motion, ingeniously transforms a simple rotational input into a lifelike stepping pattern. This mechanism, characterized by its single degree of freedom (DOF) and an eleven-link leg configuration, adeptly converts the circular motion of a crank into the linear gait of a walk. Its design is both scalable and energy-efficient, offering low payload capacity while ensuring a predictable path for each footstep. The key advantage of the Jansen mechanism lies in its simplicity and effectiveness, making it a preferred choice for implementing walking motions in the field of legged robotics.

Recently, Wu et al. [5] introduced the development of a novel closed-chain elastic-bionic leg (CEL) mechanism, which incorporates a single actuated DOF inspired by the spring-loaded inverted pendulum (SLIP) model. This innovation aims to improve the efficiency of leg mechanisms in robotic applications, focusing on simple control, enhanced stiffness, and the capability for full rotation driving. The design features an eight-bar linkage that mimics the muscular and skeletal structure of a cheetah's leg, targeting optimal performance in high-speed conditions. By employing kinematic analysis, the study establishes a link between foot trajectory, ground reaction forces, and driving forces, further examining the stiffness changes in the support phase using an equivalence model. Simulation efforts were undertaken to evaluate key parameters such as movement velocity, spring deformation, and the dynamics of running gait, leading to the creation and treadmill testing of a

prototype. This research demonstrates the potential of applying biomechanical insights to the design of robotic leg mechanisms, specifically for achieving efficient high-speed locomotion.

The present work focuses on a six-bar linkage mechanism with single DOF, originally proposed by Shieh at al. [6], which integrates a skew pantograph within its planar structure. The authors of this study have developed a new class of sixbar linkages with symmetrical coupler-point curves, enhancing the traditional four-bar linkage mechanisms. This new class of mechanisms integrates a four-bar linkage with an additional dyad to create what they describe as an embedded regular or skew pantograph. The main advantage of this design is the amplification of the coupler curve generated at the output point as compared to a standard four-bar linkage. The amplified output results in a mechanism that, while compact, offers a relatively large coupler curve. The novel structure arrangement allows for easier analysis and synthesis, facilitating the creation of these mechanisms to suit specific needs. Shieh et al. point out that these six-bar linkages are more adaptable than the typical four-bar mechanisms due to their embedded skew pantographs, which afford greater design flexibility. In their concluding remarks, they emphasize the ability of these new mechanisms to generate large symmetrical coupler curves and highlight the potential behind their development for generating the coupler curves of a four-bar linkage and a pantograph into one. The article concludes that the amplified coupler curves achieved through this integrated mechanism can be easily tailored from a regular to a skewed pantograph, offering different transmission characteristics and adhering to the same angle constraints. Finally, they provide an example of a six-bar mechanism to illustrate its compactness and efficiency in comparison to a four-bar linkage with a corresponding coupler curve, underscoring the practical advantages of their research in mechanical design and engineering.

In this study, GIM software [7], [8], [9] is utilized for the dimensional synthesis of the proposed leg mechanism, enabling the generation of an accurate foot trajectory. Once the dimensions of the mechanism are optimized, a detailed kinematic analysis is performed using GIM to simulate the leg's motion, including its trajectory, velocity, and acceleration profiles. These simulations provide valuable insights into the kinematic behavior of the mechanism. Furthermore, SolidWorks is used to conduct stress analysis and perform topology optimization on the leg mechanism, reducing its weight while maintaining structural integrity. Additionally, a prototype of the mechanism was created using 3D printing and tested to validate its functionality. This walking leg mechanism demonstrates significant potential for practical applications across various domains, including industrial operations, all-terrain vehicles, and agriculture, highlighting its versatility and capability to enhance robotic mobility in challenging environments.

2. Description of the proposed mechanism

Figure 1 illustrates the planar six-bar mechanism with a single degree of freedom, featuring an integrated skew pantograph. This mechanism represents an advanced kinematic chain widely used in various engineering fields due to its ability to accurately transmit and scale motion. Unlike traditional pantographs, this design includes additional linkages that allow it to generate more complex motion paths, even enabling three-dimensional movements. One key advantage of the six-bar skew pantograph is its ability to adjust input movements by either amplifying or reducing them through changes in the lengths and motions of its bars. This makes it highly valuable in applications requiring flexible motion outputs [10]. The mechanism's precision is particularly important in fields like precision engineering, where accurate replication of motion is critical. This level of accuracy is achieved through careful design and manufacturing processes [11], [12], [13]. Furthermore, the six-bar linkage offers great versatility, with multiple configurations available to meet different motion requirements, making it highly applicable across various technological applications [14].

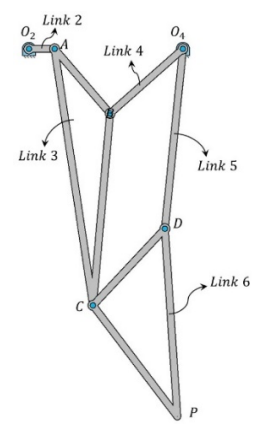


Fig. 1: Scheme of the proposed mechanism.

The primary reason for choosing this design is its ability to produce amplified and symmetrical four-bar coupler curves at the output point. This feature is especially beneficial for applications like walking machine leg mechanisms, where a

compact design with a relatively large output coupler curve is required [15]. Additionally, the leg is designed to replicate the trajectory of an amphibious leg, which is characterized by a linear supporting phase. As highlighted earlier, the proposed mechanism generates a foot path with significant height, denoted as h_p (Figure 2). This elevated foot path not only enables the reciprocal motion of the crank link but also allows the walking machine to effectively step over obstacles.

This mechanism is driven by the input link 2 (O_2A) . The four-bar linkage is denoted (O_2ABEO_4) while the embedded pantograph is (O_4BCD) . Link 6 (CDP) serves as an output link with point of contact P called foot point.

With this embedded pantograph connected to the four-bar linkage at the fictious coupler point E, the coupler curve is amplified by a factor of n, and rotated by an angle β at point P. Here, $n = O_4 D/O_4 B$ and $\beta = CDP$. On the foot-path, the distance between the two extreme positions is referred to as the horizontal stride S_P , as shown in Figure 2.

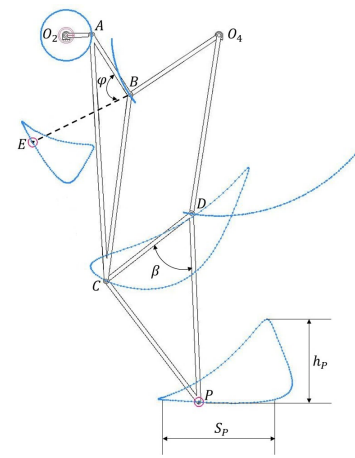


Fig. 2: Construction of Skew pantograph Mechanism using GIM software.

3. Kinematic Analysis

Kinematic analysis plays a crucial role in the conceptual design and development of robot mechanisms [16], [17], [18], [19], as it ensures that motion is precise, stable, and efficient. In this study, the dimensional synthesis is performed using GIM software [7], [9], enabling the achievement of the foot trajectory illustrated in Figure 2. This trajectory is essential for several reasons: it ensures sufficient ground clearance during the swing phase to avoid obstacles, maintains the robot's stability, and minimizes energy consumption by optimizing the path. Additionally, the smooth curve reduces impact forces during landing, ensuring consistent and controlled foot movements, which are crucial for efficient and reliable walking robot performance. The obtained foot trajectory is comparable to existing designs like the Klann's and Jansen's mechanisms, which are commonly used for such applications. The optimized leg mechanism dimensions are listed in Table 1.

Table 1: Optimized dimensions of the proposed leg mechanism.

Link Number	Denotation	Length (m)	\varphi (rad)	\beta (rad)	n
1	$O_{2}O_{4}$	d = 0.251			
2	O_2A	a = 0.0418			
		AB = 0.158			
3	ABC	BC = f =			
		0.307	1.6	0.816	1.94
4	O_4B	b = 0.158			
5	O_4D	f = 0.307			
6	DCP ¹	DP = f =			
		0.307			

The foot of a walking robot is the component that directly contacts the ground, as shown in Figure 3. With the crank's rotation, the foot follows a cyclical path relative to the walker's body, referred to as the locus. This locus is segmented into four phases: support, lift, return, and lower. During the support or stride phase, the foot maintains ground contact.

In the lift phase, the foot attains its peak height above the ground while moving in the same direction as the walker's body. Finally, the foot descends and re-establishes contact with the ground.

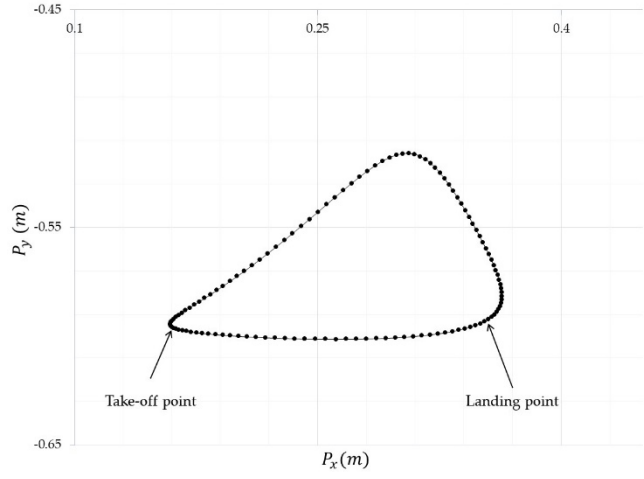
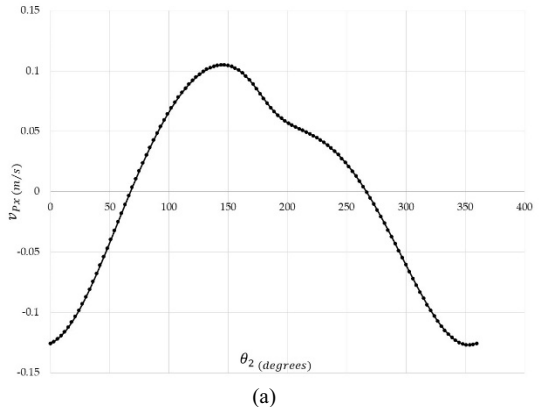
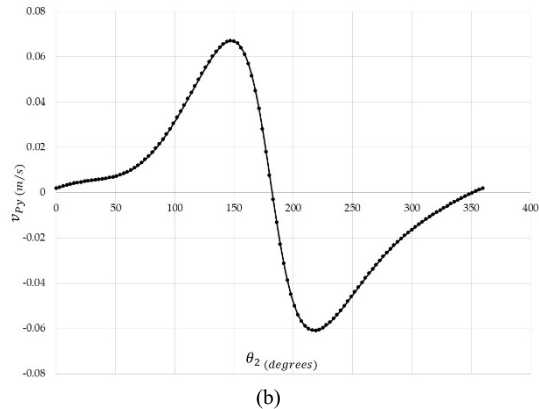


Fig. 3: Path of motion of the foot point

This trajectory is crucial for ensuring sufficient ground clearance during the swing phase to avoid obstacles, maintaining the robot's stability, and minimizing energy consumption by optimizing the path. Additionally, the smooth curve reduces impact forces during landing, ensuring consistent and controlled foot movements, which are vital for efficient and reliable walking robot performance. The start and end of the stride are characterized by more pronounced curves, facilitating a controlled descent of the foot and preventing it from scraping against the ground during elevation. The smooth, continuous curve signifies harmonic motion, further emphasizing the precision required in the foot point's trajectory for optimal robotic walking performance.

Figures 4 and 5 present the velocity and acceleration results of the foot point P in both the 'X' and 'Y' directions through kinematic analysis of the proposed mechanism. In Figure 4, the velocity of the foot point P in the 'X' direction (V_{px}) and the 'Y' direction (V_{py}) is shown. The velocity in the x direction reaches a maximum of approximately 0.11 m/s, while in the y direction, it peaks slightly near 0.065 m/s. This indicates a balanced motion in both horizontal and vertical directions. Figure 5 depicts the acceleration of the foot point P in the 'X' direction (a_{px}) and the 'Y' direction (a_{py}). The acceleration in the x direction reaches up to 0.145 m/s², while in the y direction, it shows a significantly larger peak, going up to nearly 0.21 m/s².





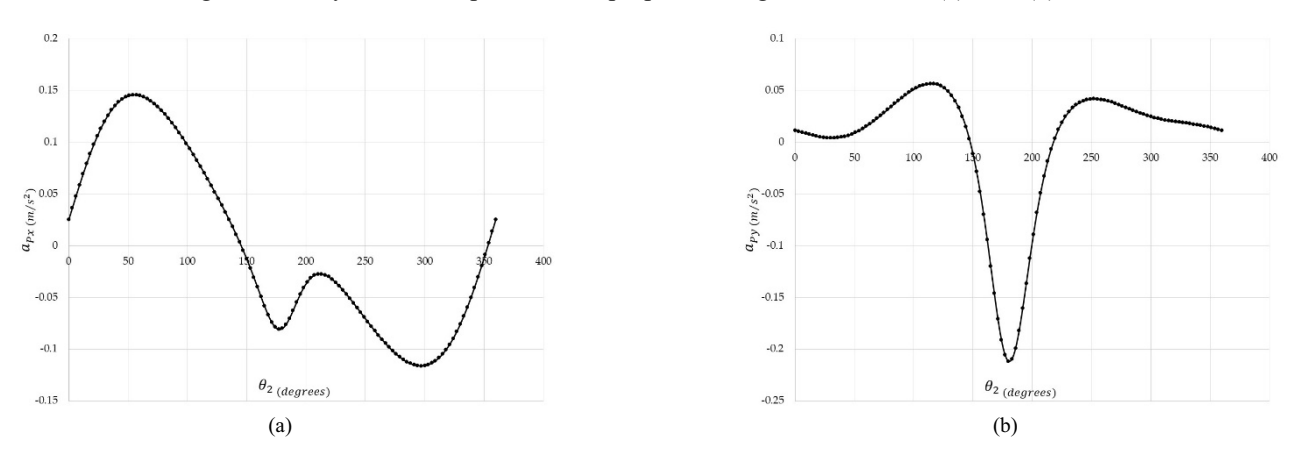


Fig. 4: Velocity of the foot point for the proposed design in directions: (a) 'X". (b) 'Y'.

Fig. 5: Acceleration of the foot point for the proposed design in directions: (a) 'X". (b) 'Y'.

The maximum velocity observed from the simulations is approximately 0.11 m/s, and the acceleration range extends up to 0.21 m/s². These values suggest that the proposed mechanism can achieve moderate speeds and accelerations, which are beneficial in reducing drag forces when interacting with surfaces like water. For ground surfaces, assuming no slip, the velocity of the feet is effectively the same as the velocity of the robot, ensuring stable and consistent movement.

4. Robot Architecture

4.1. Topology optimization

Topology optimization is performed on link 6 to reduce the weight of the leg. Figure 6 shows the different steps of this approach. The original dimensions of the part are obtained from the kinematic study, shown in Figure 6(a). This design is then modified to suit the aesthetics of the robot leg and achieve some weight reduction. A topology optimization study is then per-formed in SolidWorks to optimize the strength-to-weight ratio. The result of topology optimization serves as a guide for further removing sections from the part to arrive at the final design (Figure 6(c)).

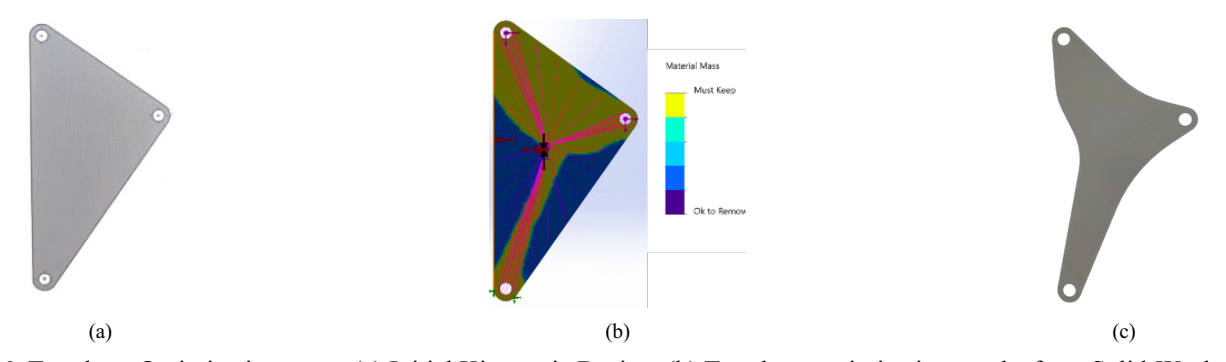


Fig. 6: Topology Optimization steps: (a) Initial Kinematic Design, (b) Topology optimization results from Solid-Works, and (c) Final Optimized Design.

4.2. Leg static analysis

The robot is designed to have a total weight of 50N, including the payload. For simulation purposes, it is assumed that the load is equally distributed across the four legs, resulting in a 10N load applied to each foot in the downward direction. The input link is driven at a speed of 10 rpm, and a motion study is conducted using SolidWorks to determine the internal forces within the system. Subsequently, a stress simulation is performed on each link throughout one complete cycle of

operation, utilizing the motion loads derived from the previous step. The cycle is divided into 25 evenly spaced sampling points, at which SolidWorks calculates the stresses generated within the model. This data is used to identify the critical position on each link where the maximum von Mises stress occurs. The link design is then modified at this critical position, while maintaining the constant length of the link, until the minimum factor of safety requirement is satisfied. These steps are repeated for each link to achieve the final design. Figures 7 to 9 shows examples of critical positions where the stresses were found to be maximum for different links, and Table II shows the corresponding von Mises stress values and the minimum factor of safety (FOS).

Table 2: Von Mises stress values and the minimum factor of safety (FOS).

Link	Maximum Stress (Pa)	Minimum FOS	
2	6.271E+06	7.89	
3	1.32E+07	3.725	
4	8.137E+06	6.08	
5	1.178E+07	4.2	
6	5.56E+06	8.9	

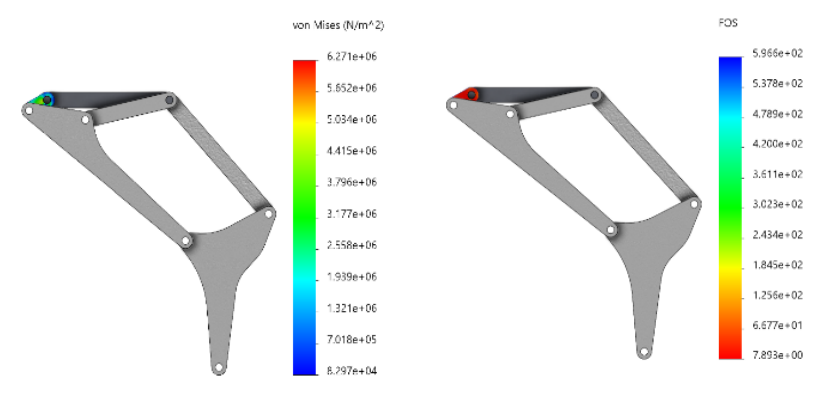


Fig. 7: Von Mises Stress and Factor of Safety of link 2

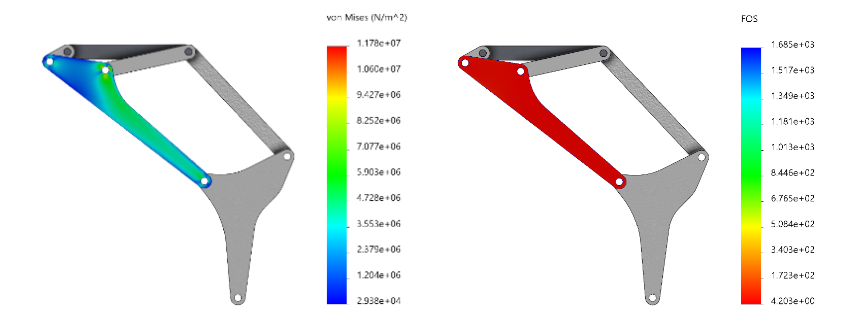


Fig. 8: Von Mises Stress and Factor of Safety of link 5

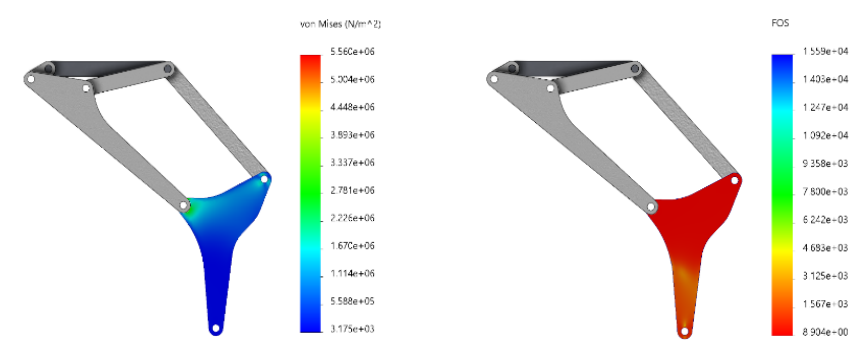


Fig. 9: Von Mises Stress and Factor of Safety of link 6

4.2. Robot system structure

In order to determine the practical accuracy of the leg mechanism, a four-legged walking machine is designed, as shown in Figure 10(a) and (b). The walking machine features a lightweight aluminum frame on which four legs are mounted (Figure 11). All the links are 3D-printed using the Ultimaker 2 Extended+ 3D printer, chosen for its high precision and reliable performance. Polylactic Acid (PLA) plastic, with a density of 1.24 g/cm³, is utilized, with optimized printing parameters such as a 0.2 mm layer height and 20% infill density to ensure structural integrity. Special attention is given to critical areas like joint connections by increasing the infill density to 50%. The 3D printing process involves the individual fabrication of components for quality control, allowing immediate testing of tolerances and ensuring precise hole alignments for smooth operation. Each leg of the robotic dog is actuated by a NEMA17 stepper motor, which is controlled via an Arduino Uno microcontroller interfaced with a CNC shield. To obtain maximum torque output, the stepper motors are configured to operate in full-step mode. This comprehensive prototyping approach validates the design objectives, ensuring the mechanism achieves enhanced stability and performance with minimal fixed pivots, providing a significant advantage over traditional designs.

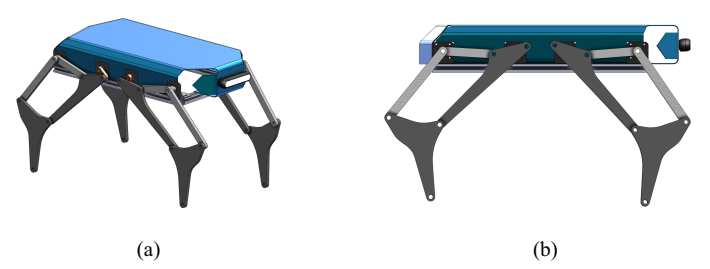


Fig. 10: CAD design of the proposed walking robot



Fig. 11: Walking machine real model

5. Conclusion

The proposed six-bar linkage mechanism with an integrated skew pantograph offers a compact and efficient solution for robotic leg mechanisms. Its design provides amplified and symmetrical foot trajectories, enabling high ground clearance and obstacle negotiation. The kinematic and stress analysis results confirm the mechanism's stability, smooth motion, and durability under varying conditions. Furthermore, the topology optimization reduced the mechanism's weight while maintaining its strength. This mechanism demonstrates significant potential for practical applications, such as walking robots and all-terrain vehicles, due to its simplicity, reliability, and adaptability. Future work could focus on refining the design for specific industrial needs and exploring its performance in dynamic environments.

Acknowledgements

The authors wish to acknowledge Erik Macho, Alfonso Hernández, CompMech, Department of Mechanical Engineering, UPV/EHU, for the permission to use the GIM® software. https://www.ehu.eus/compmech/software/

References

- [1] S. G. Desai, A. R. Annigeri, and A. TimmanaGouda, "Analysis of a new single degree-of-freedom eight link leg mechanism for walking machine," *Mechanism and Machine Theory*, vol. 140, pp. 747–764, Oct. 2019, doi: 10.1016/j.mechmachtheory.2019.06.002.
- [2] U. Vanitha, V. Premalatha, M. Nithinkumar, and S. Vijayaganapathy, "Mechanical Spider Using Klann Mechanism," 2016. Accessed: Feb. 10, 2024. [Online]. Available: https://www.semanticscholar.org/paper/Mechanical-Spider-Using-Klann-Mechanism-Vanitha-Premalatha/861f0aa1e2d608e18e334a5564e4724e38584abd
- [3] M. Rafeeq, S. Toha, S. Ahmad, M. Yousuf, M. A. Mohd Razib, and M. Hakim, "Design and Modeling of Klann Mechanism-Based Paired Four Legged Amphibious Robot," *IEEE Access*, vol. PP, pp. 1–1, Dec. 2021, doi: 10.1109/ACCESS.2021.3135706.
- [4] S. Nansai, R. E. Mohan, and M. Iwase, "Speed Control of Jansen Linkage Mechanism for Exquisite Tasks," *Journal of Advanced Simulation in Science and Engineering*, vol. 3, pp. 47–57, Aug. 2016, doi: 10.15748/jasse.3.47.
- [5] J. Wu, L. Guo, S. Yan, Y. Li, and Y. Yao, "Design and performance analysis of a novel closed-chain elastic-bionic leg with one actuated degree of freedom," *Mechanism and Machine Theory*, vol. 165, p. 104444, Nov. 2021, doi: 10.1016/j.mechmachtheory.2021.104444.
- [6] W.-B. Shieh, L.-W. Tsai, S. Azarm, and A. L. Tits, "A New Class of Six-Bar Mechanisms With Symmetrical Coupler Curves," *Journal of Mechanical Design*, vol. 120, no. 1, pp. 150–153, Mar. 1998, doi: 10.1115/1.2826668.
- [7] V. Petuya, E. Macho, O. Altuzarra, C. Pinto, and A. Hernandez, "Educational software tools for the kinematic analysis of mechanisms," *Computer Applications in Engineering Education*, vol. 22, no. 1, pp. 72–86, 2014, doi: 10.1002/cae.20532.
- [8] E. Macho, M. Urízar, V. Petuya, and A. Hernández, "Improving Skills in Mechanism and Machine Science Using GIM Software," *Applied Sciences*, vol. 11, no. 17, Art. no. 17, Jan. 2021, doi: 10.3390/app11177850.
- [9] M. AlJaimaz, Z. AlMazidi, H. AlDousari, F. Ebrahem, D. AlZayyan, and E. Gazo Hanna, "Kinematic Analysis of a Variable Speed Deep Drawing Press Using GIM Software," in *Proceedings of the 9th World Congress on Mechanical, Chemical, and Material Engineering (MCM'23)*, Aug. 2023. doi: 10.11159/icmie23.142.
- [10] J. Lenarčič and M. M. Stanišić, Eds., *Advances in Robot Kinematics: Motion in Man and Machine*, 2010th edition. Dordrecht Heidelberg: Springer, 2010.
- [11] S. Amine and E. Gazo Hanna, "Kinematic Analysis of HALF Parallel Robot," *Journal of Engineering Science and Technology Review*, vol. 12, pp. 207–213, Oct. 2019, doi: 10.25103/jestr.125.23.
- [12] R. Norton, Design of Machinery, 6th edition. New York, NY: McGraw Hill, 2019.
- [13] M. H. Chamas, S. Amine, E. Gazo Hanna, and O. Mokhiamar, "Control of a novel parallel mechanism for the stabilization of unmanned aerial vehicles," *Applied Sciences*, vol. 13, no. 15, p. 8740, 2023.
- [14] J. John J. Uicker, G. R. Pennock, and J. E. Shigley, "Theory of Machines and Mechanisms," Higher Education from Cambridge University Press.

- [15] G. R. Pennock and A. Israr, "Kinematic analysis and synthesis of an adjustable six-bar linkage," *Mechanism and Machine Theory*, vol. 44, no. 2, pp. 306–323, Feb. 2009, doi: 10.1016/j.mechmachtheory.2008.04.007.
- [16] S. Amine, L. Nurahmi, P. Wenger, and S. Caro, "Conceptual design of Schoenflies motion generators based on the wrench graph," presented at the Proceedings of the ASME Design Engineering Technical Conference, 2013. doi: 10.1115/DETC2013-13084.
- [17] E. Gazo-Hanna, A. Saber, and S. Amine, "Design and Modeling of a Six-Bar Mechanism for Repetitive Tasks with Symmetrical End-Effector Motion," *Engineering, Technology & Applied Science Research*, vol. 14, no. 5, pp. 16302–16310, 2024.
- [18] S. Amine, M. T. Masouleh, S. Caro, P. Wenger, and C. Gosselin, "Singularity analysis of the 4 RUU parallel manipulator using Grassmann-Cayley algebra," *Transactions of the Canadian Society for Mechanical Engineering*, vol. 35, no. 4, pp. 515–528, 2011, doi: 10.1139/tcsme-2011-0031.
- [19] S. Amine, S. Caro, and P. Wenger, "Constraint and singularity analysis of the Exechon," *Applied Mechanics and Materials*, vol. 162, pp. 141–150, 2012, doi: 10.4028/www.scientific.net/AMM.162.141.